

Topology across the finite temperature transition studied by overimproved cooling in gluodynamics and QCD

V. G. Bornyakov

*Institute for High Energy Physics, 142 281 Protvino, Russia
and Institute of Theoretical and Experimental Physics, 117259 Moscow, Russia*

E.-M. Ilgenfritz

Joint Institute for Nuclear Research, VBLHEP, 141980 Dubna, Russia

B. V. Martemyanov

*Institute of Theoretical and Experimental Physics, 117259 Moscow, Russia
National Research Nuclear University MEPhI, 115409, Moscow, Russia
Moscow Institute of Physics and Technology, 141700, Dolgoprudny, Moscow Region, Russia*

V. K. Mitrjushkin

*Joint Institute for Nuclear Research, BLTP, 141980 Dubna, Russia
and Institute of Theoretical and Experimental Physics, 117259 Moscow, Russia*

M. Müller-Preussker

Humboldt-Universität zu Berlin, Institut für Physik, 12489 Berlin, Germany

(Dated: April 3, 2013)

Gluodynamics and two-flavor QCD at non-zero temperature are studied with the so-called overimproved cooling technique under which caloron solutions may remain stable. We consider topological configurations either at the first occurring stable plateau of topological charge or at the first (anti)selfdual plateau and find the corresponding topological susceptibility at various temperatures on both sides of the thermal transition or crossover. In pure gluodynamics the topological susceptibility drops sharply at the deconfinement temperature while in full QCD it decreases smoothly at temperatures above the pseudocritical one. The results are close to those calculated by other methods. We interpret our findings in terms of the (in)stability of calorons with non-trivial holonomy and their dyon constituents against overimproved cooling.

PACS numbers: 11.15.Ha, 12.38.Gc, 12.38.Aw

Keywords: Lattice gauge theory, phase transition, caloron, dyon, cooling

I. INTRODUCTION

Topological charge has many faces. It is well known that the appearance of its space-time distribution strongly depends on the method by which it is studied. If resolved by means of the modes of a lattice Dirac operator with maximal chiral symmetry (the overlap Dirac operator), the resolution can be dialled by the cutoff applied to the eigenvalues of the modes (in a symmetric band enclosing the zero eigenvalue) included in that analysis. In this way very different types of topological structures are revealed, ranging from globally extended, laminar sheets of alternating sign to instanton-like lumps appearing in the infrared (IR) [1–5]. To some extent the scale of ultraviolet filtering can be mimicked by the number, say, of overimproved stout link smearing steps [4]. Before the fermionic methods became popular, only cooling [6] and smearing [7] were available for investigating the topological vacuum structure. This search was biased in favor of detecting instantons. Results concerning the “instanton structure” have been presented and discussed in the “Confinement and Topol-

ogy” sessions at the annual Lattice conferences until 2000 [8–10]. Beginning from 1998, for non-zero temperature calorons with non-trivial holonomy and their dyon constituents [11–15] have attracted more and more interest, although within a relatively small community [16–29].

There was always the hope to elucidate the different phases, both of pure Yang-Mills theory and of full QCD, in terms of the topological structure. The local behavior of the laminar sheets (and the resulting two-point function seen with few cooling steps [4, 30]), however turned out to be not critically dependent on the phase. Only in the IR, at best, the characteristic differences may become visible [31, 32]. One prominent example is the space-time anisotropy of the susceptibility in slab-like subvolumes [33] originally predicted in the instanton-antiinstanton molecule model [34].

In this paper we will use a specific (overimproved) kind of cooling [22, 35], however in the Cabibbo-Marinari mode for $SU(3)$, and we are going to use it far beyond the point where the IR structure (as a mixture of instantons and antiinstantons) usually has

been studied. Actually, this kind of action (see Eq. (2) below) was invented [35] exactly for stabilizing instantons or sphalerons [35, 36] under cooling. A similar purpose has been pursued in Ref. [22] in order to study the elusive instanton constituents at $T = 0$.

We will concentrate on the non-zero temperature case. We employ overimproved cooling in order to see in as far – after eliminating all short-range fluctuations – the emerging topological objects (“multi-caloron” configurations) will clearly distinguish between the different phases or thermodynamic states in the neighbourhood of the deconfinement transition for gluodynamics and crossover for two-flavor QCD, respectively. The nature of these topological configurations in the case of $SU(3)$ gauge theory has been carefully considered already in Ref. [24], and earlier for $SU(2)$ gauge theory in Ref. [16].

In this stadium of cooling the fields are either self-dual or anti-self-dual or trivial throughout the lattice, i.e. cooling has been employed until it reaches the scale set by the whole lattice. Hence no more details than the total topological charge Q can be read off and be associated to the original, thermalized configuration. This identification is convincing, however, since the topological charge mostly stabilizes after a few cooling steps. No further localization [32, 37] of topological charge characterizing the original Monte Carlo configurations is possible in the final stadium of cooling.

Our study instead focuses on the following questions: Under which circumstances nontrivial topological structures are stabilized with respect to cooling? How does this depend on the confining / deconfining nature of the ensemble the gauge field configurations are taken from? What is the influence of the average Polyakov loop on the result of cooling?

Our previous caloron studies [16, 24], starting from thermalized (Monte Carlo) lattices at strong coupling or deep in the confinement phase, did not consider the role of temperature in detail. Next, at an intermediate scale of resolution, the study of topological objects in $SU(2)$ lattice fields at non-zero temperature [25, 26, 28] has shown the profound difference between the confinement and deconfinement phase. To be concrete, in this analysis either 50 APE smearing steps with a smearing parameter 0.45 [25] or an overlap fermion analysis based on 20 lowest modes [26, 28] have been applied.

The following picture of the topological content of $SU(2)$ lattice gauge theory has emerged. At low temperatures one finds topological objects represented by non-dissociated calorons with maximally nontrivial holonomy [11–13]. With increasing temperature [38] their composite nature in the form of monopoles becomes recognizable. They start to dissociate into dyons of topological charge $\pm 1/2$ that appear (in the limiting case) as static $U(1)$ monopoles in the maximally Abelian gauge. Approaching the transition tem-

perature T_c (to the deconfining phase) from below, approximately one half of the calorons were observed dissociated, retaining the symmetry between the constituent dyons.

Above the transition temperature, a non-zero expectation value of the averaged Polyakov loop develops, which induces an asymmetry between the constituent dyons. This can be comprehensively explained in terms of the peak values of the local Polyakov loop [28]: “light” (anti)dyons, with the local Polyakov loop of same sign as the averaged (prevailing background) Polyakov loop, become the most abundant topological objects, while “heavy” dyons or antidyons with the local Polyakov loop opposite to the average are suppressed [39, 40]. The former “heavy” dyons may still carry highly localized fermionic zero modes bound to the “defects” detectable in the local Polyakov loop [41, 42]. Nondissociated calorons are even more suppressed.

First steps towards the statistical mechanics of self-dual dyons for the case of $SU(2)$ gauge theory, supposed to be valid in the region around the critical temperature and derived from the semiclassical partition function, have been made in the papers [43, 44].

The present paper does not attempt to consider topology at the above mentioned intermediate scale of resolution. Concerning $SU(3)$ gauge theory, this is left to an overlap fermion analysis of gauge field configurations which is in progress. The main outcome of the present study will be that the phase transition between confinement and deconfinement in $SU(3)$ gluodynamics can also be characterized by the sharp change in the appearance of topological objects remaining once cooling has hit the lattice scale. We confront this with corresponding (softer) results for the crossover known to replace the phase transition in the case of full QCD with $N_f = 2$ dynamical fermions.

We claim that our observations concerning the behavior of action and Polyakov loop can be explained by the dyonic structure of calorons. We investigate the volume and discretization effects for the topological susceptibility calculated by the use of topological charges measured either at plateaus of topological charge or identified by the coincidence between $|Q|$ and S/S_{inst} and compare it with the topological susceptibility of uncooled Monte Carlo configurations calculated by other methods [45–47].

The following Section II contains the main definitions as well as some details of the simulations we have used here or where the full QCD configurations are taken from. Section III shows examples of cooling histories for $SU(3)$ gluodynamics in the confined and deconfined phases. We comment on the influence of the overimprovement parameter. The temperature dependence of the calculated topological susceptibility, both for pure gauge theory and for QCD, is discussed in Section IV. In Section V the evolution of the averaged Polyakov loop during the cooling process for

$SU(3)$ gluodynamics and for full QCD, both in the confined and deconfined phases, is presented and the interpretation with the help of the dyonic picture of the gauge field ensemble is discussed. Section VI is reserved for conclusions and discussion. In the Appendix we recall some facts on $SU(3)$ calorons and dyons.

II. THERMAL ENSEMBLES

For the study of the phase transition in the $SU(3)$ pure gauge theory we employ the standard Wilson action S_W with the lattice coupling $\beta = 6/g_0^2$ where g_0 is the bare coupling constant. To determine the corresponding lattice spacing a as a function of β , for this action we have used the Necco–Sommer parametrization [48]. In what follows we will refer to this case as *gluodynamics*.

To study the topological aspects of the phase transition or crossover in a theory with dynamical quarks we have studied gauge field configurations generated with the gauge action S_W and $N_f = 2$ dynamical flavors of nonperturbatively $O(a)$ improved Wilson fermions (clover fermions). The configurations had been produced by the DIK collaboration [49] using the Berlin QCD code (BQCD) [50]. The improvement coefficient c_{SW} was determined nonperturbatively [51]. The lattice spacing and pion mass has been determined by interpolation of $T = 0$ results obtained by QCDSF [52]. In the remainder of the paper this case will be referred to as *full QCD*.

Our calculations were performed on asymmetric lattices with the four-dimensional volume $V = a^4 L_t \cdot L_s^3$, where L_t is the number of sites in the time ($4th$) direction. The temperature T is given by $T = 1/aL_t$. In the case of gluodynamics we have employed $L_t = 4$, $L_s = 16$ as well as $L_s = 24$ lattices, for which we have generated and analyzed 1000 and 500 configurations, respectively, at a set of β values. The coupling $\beta_c = 5.692$ [53] characterizes the transition at $L_t = 4$. It corresponds to the critical temperature $T_c \simeq 300$ MeV [46]. In order to study finite lattice spacing effects we have also simulated $L_t = 6$, $L_s = 24$ lattices with statistics of 500 gauge field configurations for each β value. The phase transition in this case takes place at $\beta_c = 5.894$ [53]. In order to keep autocorrelations small, all measurements were made on configurations separated by 500 sweeps.

In the case of full QCD [49] we have analysed configurations produced on lattices with $L_t = 8$ and spatial sizes $L_s = 16$ (500 configurations at each T/T_c) and $L_s = 24$ (200 configurations at each T/T_c). The temperature T was effectively varied at fixed β -value by changing the Wilson fermion hopping parameter κ , i.e. the quark mass was not kept constant. The chiral crossover temperature $T_c \approx 230$ MeV was determined

in Refs. [49, 54] at a pion mass value of $O(1 \text{ GeV})$.

III. COOLING HISTORIES

Technically, we cool down each gauge field configuration by means of the usual Cabibbo-Marinari cooling procedure, now with respect to an overimproved action [35] that has been used before [24] for the study of $SU(3)$ calorons and multicalorons. We monitor the cooling process and search for plateaus of the action and topological charge appearing in the cooling history. We consider

- either the first plateau of the topological charge, when the topological charge Q stays near some integer value n ($|Q - n| < 0.1$) for at least 100 cooling sweeps,
- or the first (anti)selfdual plateau, when the difference between $|Q|$ and the action S (measured in units of instanton action S_{inst}) becomes small ($S/S_{inst} - |Q| < 0.1$).

For both gluodynamics and full QCD in the confined phase we observe the two kinds of plateaus to coincide, whereas deep in the deconfined phase no plateaus of any kind are seen. In the transition region (just above the transition to the deconfined phase or for full QCD above the crossover) the first topological charge plateaus can be different from the first (anti)selfdual plateaus. Moreover, both plateaus are unstable.

We use overimproved cooling [35] because it partially stabilizes calorons with respect to shrinking and falling “through the meshes of the lattice”. The following parametrization of the lattice action ($\overset{\bullet}{\xrightarrow{x \mu}} \equiv U_\mu(x) \in SU(N)$ link variable) allows for over- and underimprovement [35],

$$S(\varepsilon) = \sum_{x,\mu,\nu} \frac{4-\varepsilon}{3} \text{Re Tr} \left(1 - \nu \overset{\bullet}{\xrightarrow{x \mu}} \right) \quad (1)$$

$$+ \sum_{x,\mu,\nu} \frac{\varepsilon-1}{48} \text{Re Tr} \left(1 - \nu \overset{\bullet}{\xrightarrow{x \mu}} \right).$$

Expanding in powers of the lattice spacing a one finds [35],

$$S(\varepsilon) = \sum_{x,\mu,\nu} a^4 \text{Tr} \left[-\frac{1}{2} F_{\mu\nu}^2(x) + \frac{\varepsilon a^2}{12} (\mathcal{D}_\mu F_{\mu\nu}(x))^2 \right] + O(a^8) \quad (2)$$

(note that no implicit summation convention is implied in this formula). $S(\varepsilon = 1)$ corresponds to the Wilson action, and the sign of the leading lattice artifacts is simply reversed by changing the sign of ε .

Based on a discretized continuum one-instanton solution of size ρ , one finds

$$S(\varepsilon) = 8\pi^2 \left[1 - \frac{\varepsilon}{5}(a/\rho)^2 + \mathcal{O}(a/\rho)^4 \right], \quad (3)$$

suggesting that under cooling ρ will decrease for $\varepsilon > 0$ and increase for $\varepsilon < 0$.

In order to illustrate the influence of the parameter ε , we present in Fig. 1 three cooling histories for $\varepsilon = 1$ (Wilson action), $\varepsilon = 0$ (slightly overimproved action), and $\varepsilon = -1$ (strongly overimproved action, our choice in this paper). The left panel shows this comparison for a gluodynamics configuration taken from the confined phase, the right panel for a gluodynamics configuration from the transition region. In the full statistics analysis of this paper we use $\varepsilon = -1$.

Both action and topological charge were calculated with the help of the improved lattice version of the field strength tensor [55] as $S/S_{\text{inst}} = \sum_{x,a} (E^a \cdot E^a + B^a \cdot B^a)/(16\pi^2)$ and $Q = \sum_{x,a} E^a \cdot B^a/(8\pi^2)$.

As a result, for gluodynamics in the confined phase we find calorons to be stable during extended cooling. This is well seen in the left part of Fig. 2. One notices that the modulus of the topological charge approaches some plateau very early. The action (expressed in units of instanton action) later converges towards this plateau as well. The topological charge plateau is stable, what can be understood as stability of calorons, which (in the confined phase) are appearing in the form of three finite action dyons.

For gluodynamics in the transition region (early deconfined phase), calorons which are rarely present in lattice configurations are unstable and cascading down to a trivial vacuum as it is seen in the right part of Fig. 2. The first topological charge plateau sometimes happens to be different from the first (anti)selfdual plateau (this is the case shown in the right panel of Fig. 2). In this temperature range the topological susceptibility calculated by the use of topological charges measured on the two kinds of plateaus takes different values, but the difference is never larger than 6%.

Deep in the deconfined phase, at $T/T_c = 1.8$, we have found that both topological charge and action go to zero values without any intermediate plateaus.

In what follows we will use only topological charge values determined on the first topological charge plateau. In Fig. 3 again for gluodynamics the Monte Carlo time histories of the topological charge are shown for the first 200 measurements and the histogram of these values is presented with full statistics. These results are presented for the confined phase ($T = 0.883 T_c$) in the upper part and for the deconfined phase ($T = 1.117 T_c$) in the lower part of the figure. The data indicate that the topological charges are well decorrelated.

We found very similar features of cooling plateaus in full QCD.

IV. TEMPERATURE DEPENDENCE OF THE TOPOLOGICAL SUSCEPTIBILITY

Our results for the topological susceptibility

$$\chi = \frac{1}{V} \langle Q^2 \rangle \quad (4)$$

for gluodynamics are presented in the left part of Fig. 4 for lattices $16^3 \cdot 4$ (red circles), $24^3 \cdot 4$ (blue up triangles) and $24^3 \cdot 6$ (green down triangles). Respective results for full QCD are shown in the right part of Fig. 4. They were obtained by applying cooling to the lattice ensembles of the DIK collaboration for $16^3 \cdot 8$ (red up triangles) and for $24^3 \cdot 8$ (blue down triangles).

From the left part of Fig. 4 we see that the results obtained on lattices $16^3 \cdot 4$ and $24^3 \cdot 4$ are close to each other. This means that finite volume effects are practically absent. The comparison of results from lattices $16^3 \cdot 4$ and $24^3 \cdot 6$ shows that discretization effects in the confinement phase are small while sizeable discretization effects are present in the deconfined phase. In section V we suggest an explanation of this feature. On the right panel of Fig. 4 – devoted to full QCD – one can see that χ is more or less constant below T_c and starts to decrease slowly above T_c . The data also indicates finite volume effects to be small, similarly to the gluodynamics case.

The topological susceptibility calculated in this work for gluodynamics is compared in Fig. 5 (left) with the topological susceptibility calculated by the use of the index theorem for a chirally improved Dirac operator without cooling [46]. For full QCD the comparison with results obtained by the use of the index theorem for the overlap Dirac operator [47] is presented in Fig. 5 (right). In the case of gluodynamics we find rather good agreement for all data points (uncertainties in the determination of T/T_c should be taken into account) apart from one point at $T/T_c \approx 0.95$. The most essential qualitative difference between our results and those of Ref. [46] is that our data show a sharp drop of χ at the transition while the data of Ref. [46] indicate a much smoother behavior. For full QCD the results agree in the confinement phase but disagree in the deconfinement phase.

In Fig. 6 we compare our gluodynamics results with the early results of Ref. [45] (blue up triangles). In this paper the field theoretical method was applied for measuring the two-point function of the topological density. This method circumvents the problem of defining a topological charge for each configuration and uses multiplicative and additive renormalization in order to relate the two-point function at zero momentum to the continuum topological susceptibility. The comparison is made between our results for lattices $24^3 \cdot 6$ (green down triangles) and $16^3 \cdot 4$ (red circles) and the results of Ref. [45] which refer to a $32^3 \cdot 8$ lattice (blue up triangles). The agreement with our results obtained on finer $24^3 \cdot 6$ lattices looks very

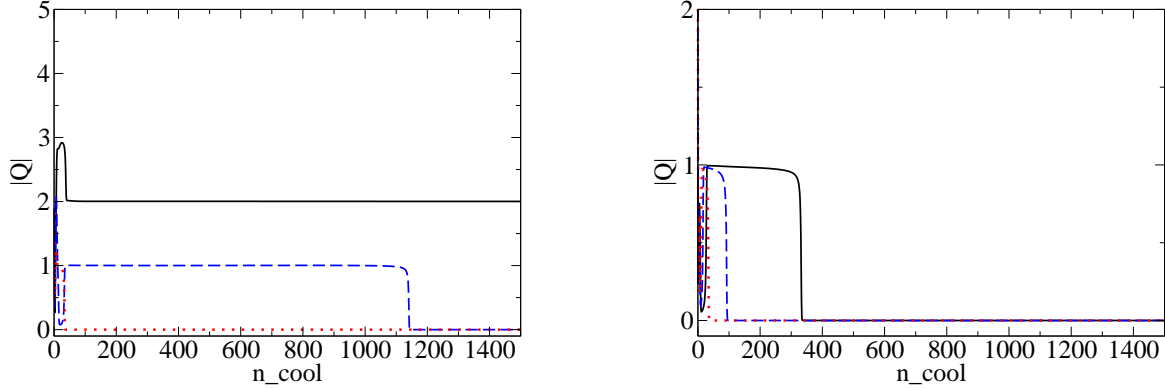


FIG. 1: Cooling histories of $|Q|$ corresponding to $\varepsilon = 1$ (Wilson action, red dotted line), $\varepsilon = 0$ (slightly overimproved action, blue dashed line) and $\varepsilon = -1$ (overimproved action as used in the rest of this paper, black solid line). Left: different cooling histories for one configuration from the confined phase. Right: different cooling histories for a (conditionally stable) caloron in a configuration taken from the transition region.

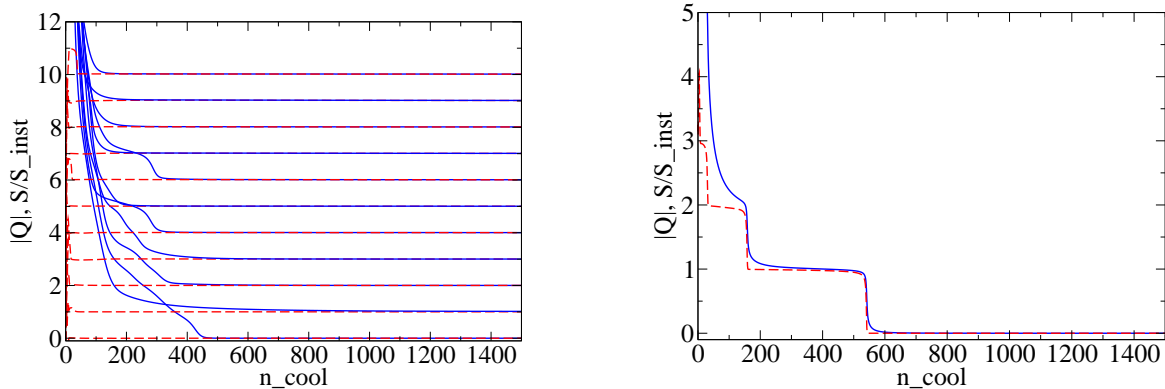


FIG. 2: Typical cooling histories of configurations from the confined phase (left). The cooling history of an (finally unstable) caloron in a configuration taken from the transition region (right). The red dashed lines represent $|Q|$, the blue solid lines represent S .

good in both phases. This could be an indication of the absence of discretization effects on our $L_t = 6$ lattices. This is supported by comparison with very recent results of Ref. [56] where few sweeps of cooling were used to evaluate the topological charge on a lattice of size $40^3 \cdot 10$.

V. INTERPRETATION IN TERMS OF A DYONIC PICTURE

Let us interpret our findings in terms of the caloron or dyon content of the gluonic field ensembles and of the behavior of the average Polyakov loop (related to the holonomy of the caloron configurations) during the cooling process.

We discuss the case of gluodynamics first. The action of a caloron does not depend on the holonomy (see Appendix and Fig. 9 for an illustration of this

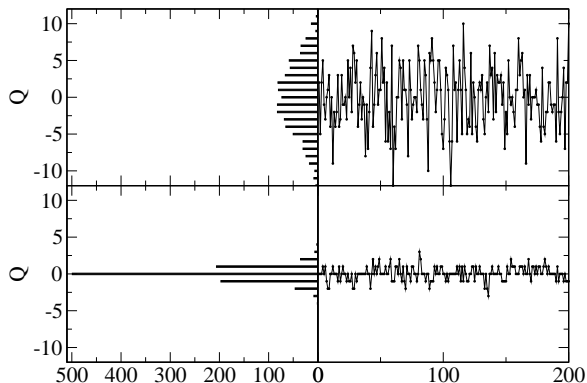


FIG. 3: The distributions of topological charges (left) and the Monte Carlo time histories along the Monte Carlo chain (right) of pure gluodynamics are shown, for the confined phase in the upper part and for the deconfined phase in the lower part. Confinement is represented by a sample at $T = 0.883 T_c$, deconfinement is illustrated by a sample at $T = 1.117 T_c$, in both cases with an actual statistics of 1000 $L_t = 4, L_s = 16$ lattice configurations (only partly shown in the history).

fact). So, while the holonomy changes considerably in the process of cooling, the action of the (multi)caloron (gradually formed in the lattice field configurations by cooling in the confined phase) is not changing. Due to this stability of the (multi)caloron action the holonomy has no preferred direction to evolve (see the left panel of Fig. 7 referring to the confined phase before and after cooling). In the deconfined phase on the other hand, even if the three center sectors are equally represented (see the right panel of Fig. 7 referring to the deconfined phase before and after cooling), under cooling the holonomy always moves towards the corresponding corner of the plot, since this is the direction where asymmetric dyon-antidyon pairs according to the experience in the $SU(2)$ case (see the Introduction) could minimize their total action.

We compare this with full QCD. In this case, center symmetry is slightly violated by the dynamical fermions already at low temperature (“confined phase”). The left panel of Fig. 8 shows where the holonomy moves to in the result of cooling. We see how the small direct violation of center symmetry in the confined phase of full QCD is amplified by cooling (again due to the effect of minimization of the action of asymmetric dyon-antidyon pairs). The right panel of Fig. 8 shows the holonomies before and after cooling in the deconfined phase. Here direct and spontaneous violation of central symmetry are summed and the asymmetry in the evolution of holonomy is more profound.

The stability of calorons in the confined phase and their partial instability in the deconfined phase, both

in the case of gluodynamics, can be understood if one takes into account that during the process of cooling the holonomy remains nontrivial in the confined phase whereas it rapidly becomes trivial in the deconfined phase. In the confined phase the caloron, for nontrivial holonomy consisting out of three localized dyons, should first form its nondissociated state by recombination of three dyons before it could “drop through the meshes”. This, however, is improbable in the process of overimproved cooling due to the repulsion between dyons [22] that the overimproved action induces.

In the deconfined phase of gluodynamics with holonomy being almost trivial in the cooling process, two light, delocalized dyons forming a caloron together with a heavy, localized dyon are already overlapping with the latter. This could be the reason of calorons being finally unstable in the deconfined phase.

In QCD, for comparison, the transition from stability to instability develops not so sharply and this is connected to the less rapid change with temperature of the evolution of the holonomy during cooling as it can be seen in Fig. 8.

As we have already seen, the comparison of results from lattices $16^3 * 4$ and $24^3 * 6$ shows the presence of sizeable discretization effects in the deconfined phase. They can be interpreted as follows. We have discussed the partial instability of calorons in the deconfined phase. It is quite natural to expect that calorons are more stable on a finer lattice where more effort is needed to let them “fall through the smaller meshes” of the lattice. Hence, on finer lattices the topological susceptibility obtained by cooling in the deconfined phase should be larger.

VI. CONCLUSIONS

In this work we have studied numerically, across the phase transition in gluodynamics and across the crossover in full QCD, the topological objects, that remain conserved or decay after a suitably chosen cooling procedure. We have applied the cooling method to find the topological content of the first topological charge plateau and of the first (anti)selfdual plateau in the cooling history of lattice configurations.

In gluodynamics, we have been able to recognize the phase transition point T_c as the point separating (within a rapid transition) temperature regions with and without surviving (anti)selfdual (topological) objects. We compare our observations for gluodynamics with full QCD with $N_f = 2$ dynamical flavors in the vicinity of the crossover temperature T_c .

We are convinced that the (anti)selfdual plateaus can be fully characterized by (multi)caloron configurations as discussed in [24]. In the rare cases, in the transition region, where the first topological charge

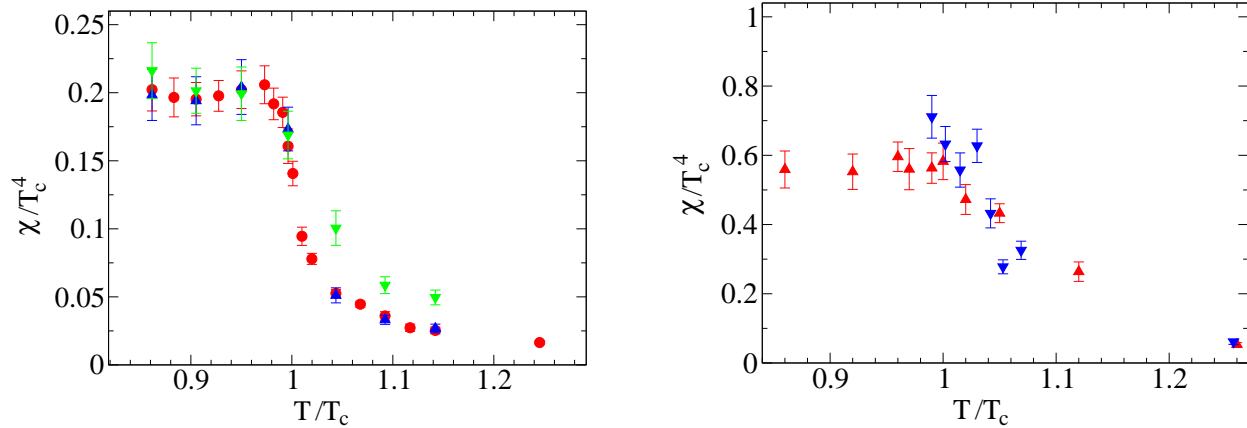


FIG. 4: Left: topological susceptibility for gluodynamics on the lattices $16^3 * 4$ (red circles), $24^3 * 4$ (blue up triangles) and $24^3 * 6$ (green down triangles). Right: susceptibility for full QCD on the lattices $16^3 * 8$ (red up triangles) and $24^3 * 8$ (blue down triangles).

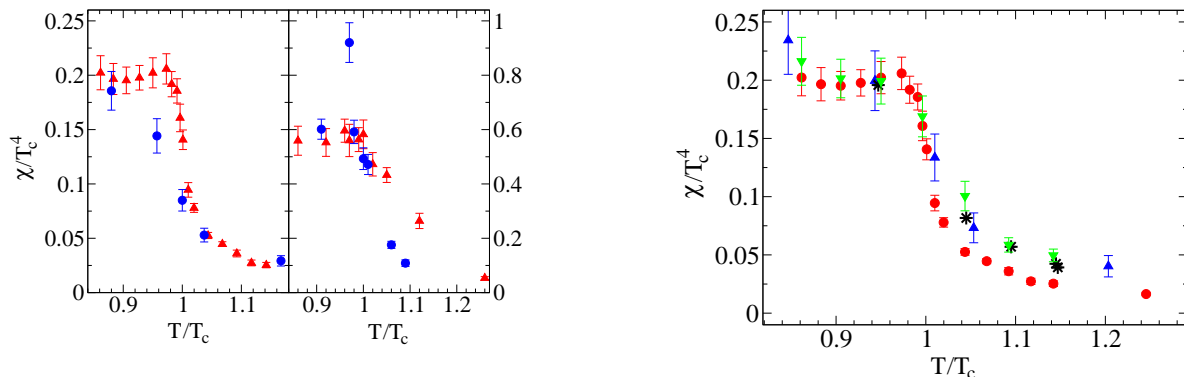


FIG. 5: Left: comparison of the topological susceptibility for gluodynamics obtained in Ref. [46] (blue circles) with the topological susceptibility calculated in the present paper (red up triangles). Right: comparison of topological susceptibility for full QCD from Ref. [47] (blue circles) with the topological susceptibility calculated in the present paper (red triangles).

plateau could differ from (anti)selfdual plateaus it is natural to assume an admixture of caloron-anticaloron or dyon-antidyon pairs.

We calculated the topological susceptibility based on the topological charges of individual lattice configurations identified in this way. We investigated the transition or crossover, respectively, from the confined to the deconfined phase with the help of this topological susceptibility χ .

In pure gluodynamics with increasing temperature, χ turned out to drop sharply down from a value close to the zero-temperature value just at the (first order) phase transition, the latter determined from the be-

FIG. 6: Comparison of the topological susceptibility for gluodynamics from Ref. [45] (blue up triangles) and from Ref. [56] (black stars) with the topological susceptibility calculated in the present paper on the lattices $24^3 * 6$ (green down triangles) and $16^3 * 4$ (red circles).

havior of the Polyakov loop or other quantities. Our finding tells us that the topological susceptibility determined via (overimproved) cooling can be used as an alternative indicator for the transition itself.

At the same time the drop off of χ could be viewed in terms of stable (multi)calorons on the confinement side and in terms of unstable dyon-antidyon pair or caloron configurations on the deconfinement side. The different behavior on both sides could be explained as triggered by the holonomy directly related to the 3-space averaged Polyakov loop for each gauge field configuration. We demonstrated that (over)improved cooling drives the holonomy to non-

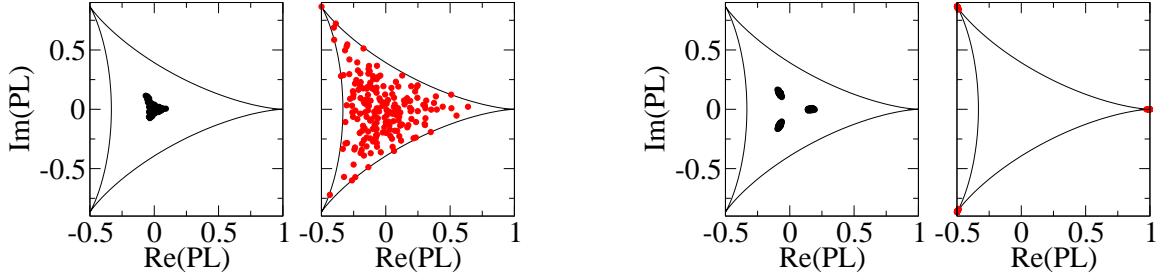


FIG. 7: For gluodynamics, scatter plots of holonomy (spatially averaged Polyakov loop) for thermalized configurations and after cooling. Left panels: for the confined phase ($T/T_c = 0.97$) and at the corresponding stable, non-trivial (anti)selfduality plateaus; right panels: for the deconfined phase ($T/T_c = 1.09$) and correspondingly after 1500 cooling sweeps at (almost) vanishing action values.

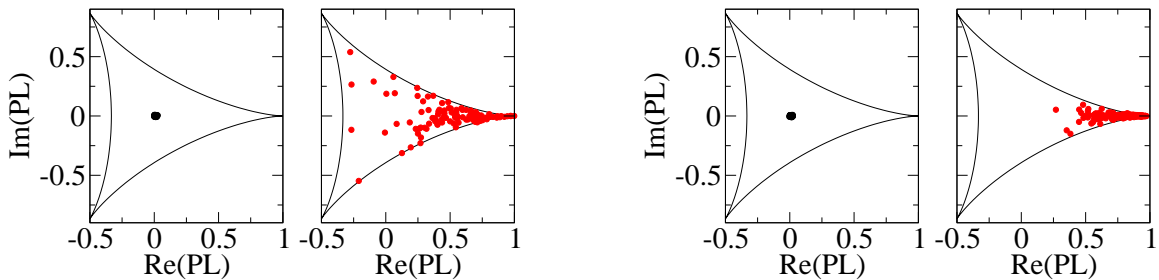


FIG. 8: For full QCD, scatter plots of holonomy (spatially averaged Polyakov loop) for thermalized configurations and after cooling at stable, non-trivial (anti)selfduality plateaus. Left panels: for the confined phase ($T/T_c = 0.96$); right panels: for the deconfined phase ($T/T_c = 1.05$).

trivial (trivial) values in the confinement (deconfinement) phase with the consequence of getting stable (unstable) (multi)caloron configurations due to their symmetric (non-symmetric) dyon content.

In full QCD the drop of the topological susceptibility turned out to be softer and to set in at a temperature that is slightly above the pseudocritical temperature T_c determined by the maximum of the Polyakov loop susceptibility [49]. Also in this case the former discussion of stable (below the crossover) or unstable (above the crossover) (multi)caloron configurations applies, since the holonomy behaves similarly in spite of the $Z(3)$ breaking effect by the dynamical fermion degrees of freedom taken into account.

We compared our results on topological susceptibilities with those of other authors employing different methods and have found a reasonable agreement.

All together, our results give us some confidence that large-scale topological objects play a major role in the change of thermal gauge field ensembles at the deconfinement phase transition in gluodynamics as well as at the crossover phenomenon in full QCD.

Acknowledgments

B.V.M. appreciates the support of Humboldt-University Berlin where the main part of the work was done. V.G.B. is supported by RFBR grant 11-02-01227-a and by grant of the Russian Ministry of Science and Education.

Appendix: $SU(3)$ calorons

The $SU(N)$ instantons at finite temperature (or calorons) with non-trivial holonomy [11–13] can be considered as composites of N constituent monopoles, seen only when the Polyakov loop at spatial infinity (holonomy) is non-trivial. In the periodic gauge, $A_\mu(t+\beta, \vec{x}) = A_\mu(t, \vec{x})$ it is defined as

$$\mathcal{P}_\infty = \lim_{|\vec{x}| \rightarrow \infty} P \exp\left(\int_0^\beta A_0(\vec{x}, t) dt\right). \quad (5)$$

After a suitable constant gauge transformation, the Polyakov loop can be characterised by real numbers $\mu_{m=1, \dots, n}$ ($\sum_{m=1}^n \mu_m = 0$) that describe the eigenval-

ues of the holonomy

$$\mathcal{P}_\infty^0 = \exp[2\pi i \text{diag}(\mu_1, \dots, \mu_n)], \quad (6)$$

$$\mu_1 \leq \dots \leq \mu_n \leq \mu_{n+1} \equiv 1 + \mu_1.$$

In units, where the inverse temperature $\beta = 1$, a simple formula for the $SU(N)$ action density can be written [11, 12] :

$$\text{Tr} F_{\mu\nu}^2(x) = \partial_\mu^2 \partial_\nu^2 \log \psi(x), \quad (7)$$

$$\psi(x) = \frac{1}{2} \text{tr}(\mathcal{A}_n \cdots \mathcal{A}_1) - \cos(2\pi t),$$

$$\mathcal{A}_m \equiv \frac{1}{r_m} \begin{pmatrix} r_m & |\vec{y}_m - \vec{y}_{m+1}| \\ 0 & r_{m+1} \end{pmatrix} \begin{pmatrix} c_m & s_m \\ s_m & c_m \end{pmatrix},$$

with $r_m = |\vec{x} - \vec{y}_m|$ and \vec{y}_m being the center of mass radii of m constituent monopoles, which can be assigned a mass $8\pi^2\nu_m$, where $\nu_m \equiv \mu_{m+1} - \mu_m$. Furthermore, $c_m \equiv \cosh(2\pi\nu_m r_m)$, $s_m \equiv \sinh(2\pi\nu_m r_m)$, $r_{n+1} \equiv r_1$ and $\vec{y}_{n+1} \equiv \vec{y}_1$.

For $SU(3)$ calorons we correspondingly parametrize the asymptotic holonomy as $\mathcal{P}_\infty^0 = \text{diag}(e^{2\pi i\mu_1}, e^{2\pi i\mu_2}, e^{2\pi i\mu_3})$, with $\mu_1 \leq \mu_2 \leq \mu_3 \leq \mu_4 = 1 + \mu_1$ and $\mu_1 + \mu_2 + \mu_3 = 0$. Let \vec{y}_1, \vec{y}_2 and \vec{y}_3 be three $3D$ position vectors of dyons remote from each other. Then a caloron consists of three lumps carrying the instanton action split into fractions $m_1 = \mu_2 - \mu_1$, $m_2 = \mu_3 - \mu_2$ and $m_3 = \mu_4 - \mu_3$, concentrated near the \vec{y}_i .

Provided the constituents are well separated, the Polyakov loop values at their positions \vec{y}_m , $m = 1, 2, 3$ are [57]

$$\mathcal{P}(\vec{y}_1) = \text{diag}(e^{-\pi i\mu_3}, e^{-\pi i\mu_3}, e^{2\pi i\mu_3}),$$

$$\mathcal{P}(\vec{y}_2) = \text{diag}(e^{2\pi i\mu_1}, e^{-\pi i\mu_1}, e^{-\pi i\mu_1}), \quad (8)$$

$$\mathcal{P}(\vec{y}_3) = \text{diag}(-e^{-\pi i\mu_2}, e^{2\pi i\mu_2}, -e^{-\pi i\mu_2}).$$

The complex numbers representing the trace of Polyakov loop $PL = \frac{1}{3}\text{Tr}\mathcal{P}$ occupy some region on the complex plane (see e.g. Fig. 7). The holonomy \mathcal{P}_∞^0 is traced to point PL_∞ that is close to (one third of) the trace of Polyakov loop averaged over all lattice points and is near zero in the confining phase and near one in the deconfining phase. There is a one-to-one correspondence between (one third of) the trace of Polyakov loop and three numbers $m_1, m_2, m_3, m_1 + m_2 + m_3 = 1$ that define the eigenvalues of $SU(3)$ matrix and hence its trace. Three numbers can be represented by the inner point of regular triangle for which the sum of the lengths of three perpendiculars to triangle sides is constant (equal to one, see Fig. 9). The region on the complex plane occupied by (one third of) the trace of Polyakov loop can be considered as some nonlinear deformation of this regular triangle. The point O on Fig. 9 corresponds to PL_∞ while points A_1, A_2, A_3 correspond to the values of (one third of) the trace of the Polyakov loop at the constituent positions (8).

-
- [1] I. Horvath, N. Isgur, J. McCune, and H. Thacker, Phys.Rev. **D65**, 014502 (2002), hep-lat/0102003.
- [2] I. Horvath, S. Dong, T. Draper, F. Lee, K. Liu, et al., Phys.Rev. **D68**, 114505 (2003), hep-lat/0302009.
- [3] E.-M. Ilgenfritz, K. Koller, Y. Koma, G. Schierholz, T. Streuer, et al., Phys.Rev. **D76**, 034506 (2007), 0705.0018.
- [4] E.-M. Ilgenfritz, D. Leinweber, P. Moran, K. Koller, G. Schierholz, et al., Phys.Rev. **D77**, 074502 (2008), 0801.1725.
- [5] H. Thacker and C. Xiong, Phys.Rev. **D86**, 105020 (2012), 1208.4784.
- [6] E.-M. Ilgenfritz, M. L. Laursen, G. Schierholz, M. Müller-Preussker, and H. Schiller, Nucl. Phys. **B268**, 693 (1986).
- [7] M. Albanese et al. (APE), Phys. Lett. **B192**, 163 (1987).
- [8] J. W. Negele, Nucl.Phys.Proc.Suppl. **73**, 92 (1999), hep-lat/9810053.
- [9] M. Teper, Nucl.Phys.Proc.Suppl. **83**, 146 (2000), hep-lat/9909124.
- [10] M. Garcia Perez, Nucl.Phys.Proc.Suppl. **94**, 27 (2001), hep-lat/0011026.
- [11] T. C. Kraan and P. van Baal, Nucl.Phys. **B533**, 627 (1998), hep-th/9805168.
- [12] T. C. Kraan and P. van Baal, Phys.Lett. **B435**, 389 (1998), hep-th/9806034.
- [13] K.-M. Lee and C.-H. Lu, Phys.Rev. **D58**, 025011 (1998), hep-th/9802108.
- [14] F. Bruckmann and P. van Baal, Nucl. Phys. **B645**, 105 (2002), hep-th/0209010.
- [15] F. Bruckmann, D. Nogradi, and P. van Baal, Nucl. Phys. **B698**, 233 (2004), hep-th/0404210.
- [16] E.-M. Ilgenfritz, B. Martemyanov, M. Müller-Preussker, S. Shcheredin, and A. Veselov, Phys.Rev. **D66**, 074503 (2002), hep-lat/0206004.
- [17] C. Gattringer, Phys. Rev. **D67**, 034507 (2003), hep-lat/0210001.
- [18] C. Gattringer and S. Schaefer, Nucl. Phys. **B654**, 30 (2003), hep-lat/0212029.
- [19] D. Diakonov, Prog. Part. Nucl. Phys. **51**, 173 (2003), hep-ph/0212026.
- [20] C. Gattringer et al., Nucl. Phys. Proc. Suppl. **129**, 653 (2004), hep-lat/0309106.
- [21] D. Diakonov, N. Gromov, V. Petrov, and S. Slizovskiy, Phys. Rev. **D70**, 036003 (2004), hep-th/0404042.
- [22] F. Bruckmann, E.-M. Ilgenfritz, B. Martemyanov, and P. van Baal, Phys.Rev. **D70**, 105013 (2004), hep-lat/0408004.
- [23] E.-M. Ilgenfritz, B. Martemyanov, M. Müller-Preussker, and A. Veselov, Phys.Rev. **D71**, 034505 (2005), hep-lat/0412028.
- [24] E. M. Ilgenfritz, M. Müller-Preussker, and D. Peschka, Phys.Rev. **D71**, 116003 (2005), hep-

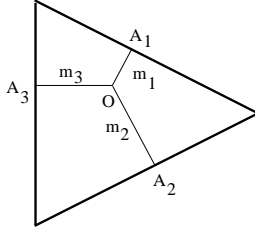


FIG. 9: The regular triangle with inner point O and three perpendiculars to triangle sides. The sum of them $OA_1 + OA_2 + OA_3 \equiv m_1 + m_2 + m_3 = 1$ is constant for all inner points.

- lat/0503020.
- [25] E.-M. Ilgenfritz, B. Martemyanov, M. Müller-Preussker, and A. Veselov, Phys.Rev. **D73**, 094509 (2006), hep-lat/0602002.
- [26] V. Bornyakov, E.-M. Ilgenfritz, B. Martemyanov, S. Morozov, M. Müller-Preussker, et al., Phys.Rev. **D76**, 054505 (2007), 0706.4206.
- [27] V. G. Bornyakov et al., PoS **LAT2007**, 315 (2007), 0710.2799.
- [28] V. Bornyakov, E.-M. Ilgenfritz, B. Martemyanov, and M. Müller-Preussker, Phys.Rev. **D79**, 034506 (2009), 0809.2142.
- [29] F. Bruckmann, E.-M. Ilgenfritz, B. Martemyanov, and B. Zhang, Phys. Rev. **D81**, 074501 (2010), 0912.4186.
- [30] F. Bruckmann, F. Gruber, N. Cundy, A. Schäfer, and T. Lippert, Phys.Lett. **B707**, 278 (2012), 1107.0897.
- [31] P. Moran and D. Leinweber (2008), 0805.4246.
- [32] P. de Forcrand, AIP Conf.Proc. **892**, 29 (2007), hep-lat/0611034.
- [33] P. de Forcrand, M. Garcia Perez, J. Hetrick, E. Laermann, J. Lagae, et al., Nucl.Phys.Proc.Suppl. **73**, 578 (1999), hep-lat/9810033.
- [34] E.-M. Ilgenfritz and E. V. Shuryak, Phys. Lett. **B325**, 263 (1994), hep-ph/9401285.
- [35] M. Garcia Perez, A. Gonzalez-Arroyo, J. R. Snippe, and P. van Baal, Nucl.Phys. **B413**, 535 (1994), hep-lat/9309009.
- [36] M. Garcia Perez and P. van Baal, Nucl.Phys. **B429**, 451 (1994), hep-lat/9403026.
- [37] Y. Koma et al., PoS **LAT2005**, 300 (2006), hep-lat/0509164.
- [38] E.-M. Ilgenfritz, B. Martemyanov, M. Müller-Preussker, and A. Veselov, Phys.Rev. **D69**, 114505 (2004), hep-lat/0402010.
- [39] V. Bornyakov, E. Lushevskaya, S. Morozov, M. Polikarpov, E.-M. Ilgenfritz, et al., Phys.Rev. **D79**, 054505 (2009), 0807.1980.
- [40] F. Bruckmann, PoS **CONFINEMENT8**, 179 (2008), 0901.0987.
- [41] F. Bruckmann, T. G. Kovacs, and S. Schierenberg, Phys.Rev. **D84**, 034505 (2011), 1105.5336.
- [42] T. G. Kovacs, F. Pittler, F. Bruckmann, and S. Schierenberg, PoS **LATTICE2011**, 200 (2011), 1112.0119.
- [43] E. Shuryak and T. Sulejmanpasic, Phys.Rev. **D86**, 036001 (2012), 1201.5624.
- [44] P. Faccioli and E. Shuryak (2013), 1301.2523.
- [45] B. Alles, M. D'Elia, and A. Di Giacomo, Nucl.Phys. **B494**, 281 (1997), hep-lat/9605013.
- [46] C. Gattringer, R. Hoffmann, and S. Schaefer, Phys.Lett. **B535**, 358 (2002), hep-lat/0203013.
- [47] V. Weinberg et al. (DIK Collaboration), PoS **LAT2007**, 236 (2007), 0710.2565.
- [48] S. Necco and R. Sommer, Phys.Lett. **B523**, 135 (2001), hep-ph/0109093.
- [49] V. Bornyakov et al. (DIK Collaboration), Phys.Rev. **D71**, 114504 (2005), hep-lat/0401014.
- [50] Y. Nakamura and H. Stüben, PoS **LATTICE2010**, 040 (2010), 1011.0199.
- [51] K. Jansen and R. Sommer (ALPHA collaboration), Nucl.Phys. **B530**, 185 (1998), hep-lat/9803017.
- [52] M. Göckeler, R. Horsley, A. Irving, D. Pleiter, P. Rakow, et al., Phys.Rev. **D73**, 054508 (2006), hep-lat/0601004.
- [53] Y. Iwasaki, K. Kanaya, T. Yoshie, T. Hoshino, T. Shirakawa, et al., Phys.Rev. **D46**, 4657 (1992).
- [54] V. Bornyakov and V. Mitrjushkin, Int.J.Mod.Phys. **A27**, 1250050 (2012), 1103.0442.
- [55] S. Bilson-Thompson, F. Bonnet, D. Leinweber, and A. G. Williams, Nucl.Phys.Proc.Suppl. **109A**, 116 (2002), hep-lat/0112034.
- [56] C. Bonati, M. D'Elia, H. Panagopoulos, and E. Vicari (2013), 1301.7640.
- [57] P. van Baal, pp. 269–279 (1999), hep-th/9912035.